Check for updates

# Optimal Design of a Damped Single Degree of Freedom Platform for Vibration Suppression in Harmonically Forced Undamped Systems

**Jimmy S. Issa**
Department of Industrial and Mechanical Engineering,
Lebanese American University,
P.O. Box 36,
Byblos, Lebanon

*Vibration reduction in harmonically forced undamped systems is considered using a new vibration absorber setup. The vibration absorber is a platform that is connected to the ground by a spring and damper. The primary system is attached to the platform, and the optimal parameters of the latter are obtained with the aim of minimizing the peaks of the primary system frequency response function. The minimax problem is solved using a method based on invariant points of the objective function. For a given mass ratio of the system, the optimal tuning and damping ratios are determined separately. First, it is shown that the objective function passes through three invariant points, which are independent of the damping ratio. Two optimal tuning ratios are determined analytically such that two of the three invariant points are equally leveled. Then, the optimal damping ratio is obtained such that the peaks of the frequency response function are equally leveled. The optimal damping ratio is determined in a closed form, except for a small range of the mass ratio, where it is calculated numerically from two nonlinear equations. For a range of mass ratios, the optimal solution obtained is exact, because the two peaks coincide with the two equally leveled invariant points. For the remaining range, the optimal solution is semiexact. Unlike the case of the classical absorber setup, where the absorber performance increases with increasing mass ratios, it is shown that an optimal mass ratio exists for this setup, for which the absorber reaches its utmost performance. The objective function is shown in its optimal shape for a range of mass ratios, including its utmost shape associated with the optimal mass ratio of the setup.* [DOI: 10.1115/1.4023811]

Downloaded from http://asmedigitalcollection.asme.org/vibrationacoustics/article-pdf/135/5/051003/6342559/vib_135_5_051003.pdf by guest on 29 May 2023

## 1 Introduction

In almost any machine, the periodic motion of mechanical parts results in applied harmonic forces, which lead, in most cases, to unwanted machine vibration. For lightly damped systems, the vibration amplitude, which is closely dependent on the forcing frequency, can reach large values when the latter is close to one of the system's natural frequencies. To overcome this problem, many techniques were proposed to control and attenuate this unwanted vibration. The vibration absorber is one of the most famous passive vibration suppression techniques. When attached to a system, this simple device can significantly reduce the vibration of its host if properly designed.

This clever idea was first patented by Frahm [1] a long time ago in 1911. Since then, vibration absorbers have been the subject of a large volume of publications. The first analytical treatment of the damped vibration absorber attached to an undamped primary system was conducted by Ormondroyd and Den Hartog [2]. The optimal absorber parameters were first determined by Den Hartog [3] in an analytical closed form using the invariant points method. The analysis is based on the existence of two points of the frequency response function that are independent of the absorber damping. First, the two points were adjusted to equal heights by a proper choice of the tuning ratio. Then, two suboptimal damping ratios were obtained by forcing the frequency response function to pass horizontally through each fixed point. The approximate optimal solution was determined from a convenient average of these two solutions. Brock [4] derived an analytical expression for the optimal damping ratio using a simple perturbation method. This classical absorber design theory can be found in vibration textbooks (e.g., Refs. [5,6]). Recently, the exact analytical solution of this problem was derived by Nishihara and Asami [7] by equally leveling the peaks of the frequency response function. It is shown that the approximate solution based on the invariant points method is highly accurate and closely matches the exact optimal solution. Snowdon [8] determined the optimal parameters using the approximate method of an absorber attached to its host with a rubberlike material. The invariant points method was extended to multidegree of freedom systems by Ozer and Royston [9].

The works cited thus far correspond to damped vibration absorbers attached to harmonically forced undamped primary systems. The frequency response function of a damped primary system coupled with a damped absorber does not exhibit invariant points. Therefore, the invariant points method cannot be used to determine the approximate optimal parameters in a closed form. Furthermore, the exact optimal solution cannot be obtained analytically, because the expression of the objective function becomes complicated. An exception is found in Asami and Nishihara [10], where hysteretic damping is present in both the primary system and absorber. Bapat and Kumaraswamy [11] determined the optimal parameters in closed form for the Lanchester damper case. In all other cases, the optimal parameters are calculated numerically for a range of the mass and damping ratios of the system, as in Thompson [12], Randall et al. [13], Soom and Lee [14], and Pennestri [15]. The numerical results were presented in ready-to-use graphs for the design of absorbers coupled to damped primary systems. Designs of absorbers with multidegrees of freedom have been proposed (e.g., Febbo and Vera [16] and Febbo [17]); the reader is referred to the references therein for a more exhaustive coverage of this aspect of the research.

Contributed by the Design Engineering Division of ASME for publication in the Journal of Vibration and Acoustics. Manuscript received May 27, 2011; final manuscript received January 30, 2013; published online June 18, 2013. Assoc. Editor: Wei-Hsin Liao.

 **Copyright © 2013 by ASME** 

In the classical absorber setup, which is shown in Fig. 1(*a*), the primary system is modeled as a mass attached to the ground by a spring and damper, and the absorber is directly coupled to the primary mass. In this setup, the absorber position on the primary system should be carefully chosen to ensure that the latter is able to withstand the absorber's weight and forces resulting from the absorber vibration. In some cases, one would fail to find a suitable attachment point for the absorber, since it results in a large concentrated load to be applied to a small area of its host structure. Delicate instruments with flimsy structures are examples of systems that cannot tolerate large loads on their external structures. For such systems, it is sometimes more suitable to have them attached to a platform, which acts as a vibration absorber. The proposed vibration absorber setup is shown in Fig. 1(*b*). The objective of this work is the determination of the optimal parameters of the new absorber setup for vibration reduction in harmonically forced undamped systems. In Sec. 2, the equations of motion are derived and the frequency response functions are written in terms of dimensionless parameters. The optimization strategy is detailed and discussed in Sec. 3. The optimal tuning and damping ratios are determined in Secs. 4 and 5, respectively. The results are discussed in Sec. 6, where the optimal mass ratio is calculated. Concluding remarks and directions for future works are given in Sec. 7.

## 2 Frequency Response Functions

A harmonically forced undamped primary system attached to a viscously damped platform is shown in Fig. 2, where $M$ and $m$ denote the primary system and absorber masses, respectively. $K$ and $k$ are the primary system and absorber stiffness constants, respectively, and $c$ is the absorber viscous-damping constant. The equations of motion of the system take the form

$$\begin{aligned} M\ddot{x} + K(x-y) &= f_0 \sin(\omega t) \\ m\ddot{y} + K(y-x) + ky + c\dot{y} &= 0 \end{aligned} \tag{1}$$

In Eq. (1), $x$ and $y$ are the displacements of the primary mass and platform, respectively, as depicted in Fig. 2. $\dot{\square}$ denotes the derivative of $\square$ with respect to time $t$, $f_0$ is the forcing amplitude, and $\omega$ its frequency. Let $\tilde{X}$ and $\tilde{Y}$ denote the steady state complex frequency response functions of the primary system and platform, respectively. $\tilde{X}$ and $\tilde{Y}$ can be easily determined from Eq. (1) as

$$\begin{aligned} \tilde{X} &= \frac{f_0(k + K - m\omega^2 + \mathbf{i}\, c\omega)}{(k - m\omega^2)(K - M\omega^2) - KM\omega^2 + \mathbf{i}\, c\omega(K - M\omega^2)} \\ \tilde{Y} &= \frac{f_0 K}{(k - m\omega^2)(K - M\omega^2) - KM\omega^2 + \mathbf{i}\, c\omega(K - M\omega^2)} \end{aligned} \tag{2}$$

In Eq. (2), $\mathbf{i}$ denotes the imaginary unit. The same dimensionless notation adopted in the classical absorber analysis in Ref. [4] is used in this work. Let $\omega_p^2 = k/m$ and $\omega_n^2 = K/M$ denote the squared natural frequencies of the platform and primary system,

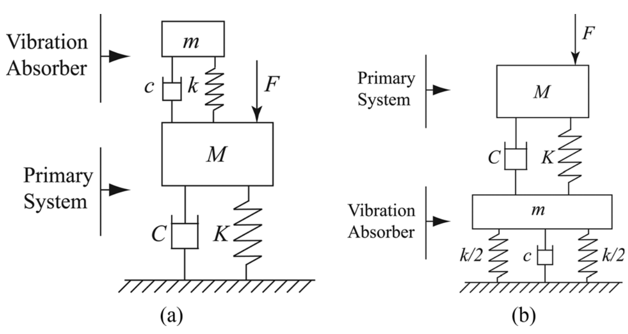


**Fig. 1 (*a*) Classical vibration absorber setup and (*b*) proposed vibration absorber setup**

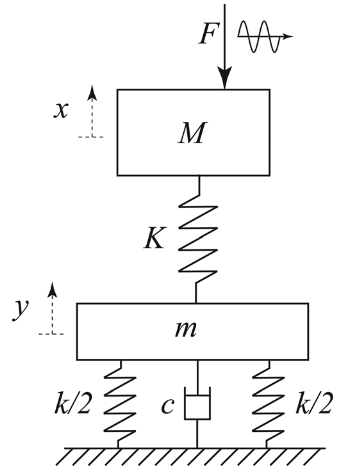


**Fig. 2 An undamped primary system attached to a viscously damped platform (absorber)**

respectively. Let $\delta_{st} = F_0/K$ denote the static deflection of the primary system when directly connected to the ground. The dimensionless parameters used are defined as follows:

$$\begin{aligned} \text{Mass ratio } \mu &= m/M\,, \\ \text{Tuning ratio } f &= \omega_p/\omega_n\,, \\ \text{Frequency ratio } g &= \omega/\omega_n\,, \\ \text{Damping ratio } \zeta &= c/2m\omega_n \end{aligned} \tag{3}$$

Now, let $X = \| \tilde{X} \|$ and $Y = \| \tilde{Y} \|$ be the norms of $\tilde{X}$ and $\tilde{Y}$, respectively. $X/\delta_{st}$ and $Y/\delta_{st}$ are written in terms of the dimensionless parameters as

$$\begin{aligned} \frac{X}{\delta_{st}} &= \sqrt{\frac{(1 + f^2\mu - g^2\mu)^2 + 4g^2\mu^2\zeta^2}{((1-g^2)(f^2-g^2)\mu - g^2)^2 + 4g^2(1-g^2)^2\mu^2\zeta^2}} \\ \frac{Y}{\delta_{st}} &= \frac{1}{\sqrt{((1-g^2)(f^2-g^2)\mu - g^2)^2 + 4g^2(1-g^2)^2\mu^2\zeta^2}} \end{aligned} \tag{4}$$

The objective of this work is the determination of the optimal absorber parameters such that the steady state response of the primary system is minimized for all forcing frequencies. This is achieved by solving a minimax problem, in which the statement reads as follows: ***For a given mass ratio* $\mu$ *of the system, determine the optimal tuning ratio* $f_{opt}$ *and damping ratio* $\zeta_{opt}$ *such that the maximum of the objective function* $X/\delta_{st}$ *is minimized* $\forall g$.**

This problem is solved using a method based on invariant points, which is similar to that used by Den Hartog for the classical absorber setup. In Sec. 3, the invariant points, which are independent of the absorber damping, are determined and the optimization procedure is detailed.

## 3 Optimization Procedure

Let $H(g) = X/\delta_{st}$ denote the objective function. Before proceeding with the solution of this problem, it is important to note special features of $H(g)$. The plots of the objective function for $\mu = 3$, $f = 0.5$, and three different values of the damping ratio $\zeta$ are illustrated in Fig. 3. The figure clearly shows the existence of three invariant points, depicted by $Q_0$, $Q_1$, and $Q_2$, which are independent of $\zeta$. The first fixed point $Q_0$ corresponds to the static deflection of the system (i.e., for $g = g_0 = 0$). The frequency ratios $g_1$ and $g_2$ associated with $Q_1$ and $Q_2$ are given in Appendix A.1. Since these fixed points are independent of the damping ratio $\zeta$, it is then imperative to find them suitable positions first by carefully choosing the tuning ratio $f$, as this will ease the optimization



Downloaded from http://asmedigitalcollection.asme.org/vibrationacoustics/article-pdf/135/5/051003/6342559/vib_135_5_051003.pdf by guest on 29 May 2023

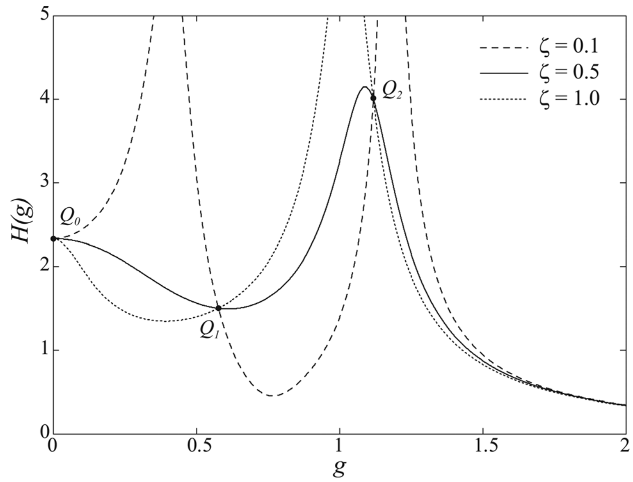


**Fig. 3 Plot of $H(g)$ for different damping ratios illustrating three invariant points depicted by $Q_0$, $Q_1$, and $Q_2$**

problem. Then, the optimal damping ratio can be determined by forcing $H(g)$ not to exceed the highest invariant point. Therefore, understanding the behavior of these points as $f$ varies is essential to correctly tune the system. To achieve that, the objective function is calculated at these points for $f=0$, and it is shown in Appendix A.2 that

$$H(g_1)|_{f=0} \geq H(g_2)|_{f=0} \quad \forall \mu \leq 1\,,$$
$$H(g_1)|_{f=0} < H(g_2)|_{f=0} \quad \forall \mu > 1\,,$$
$$H(g_0)|_{f=0} = +\infty \quad \forall \mu > 0$$

A sketch of the invariant points positions at $f=0$ is shown in Fig. 4(*a*). The rate of change of $H(g)$ with respect to $f$ is calculated at each invariant point in Appendix A.2, where it is shown that

$$\frac{\partial H(g_0)}{\partial f} < 0, \quad \frac{\partial H(g_1)}{\partial f} \geq 0, \quad \frac{\partial H(g_2)}{\partial f} \leq 0$$

The arrows in Fig. 4(*a*) indicate the direction of motion of these points as $f$ increases from zero. When $f=0$ and $\forall \mu$, $Q_0$ starts at infinity and is lowered as $f$ increases. When $\mu > 1$, $Q_1$ starts at a position lower than that of $Q_2$ and higher than or equal to that of $Q_2$ if $\mu \leq 1$, as depicted in Fig. 4(*a*). As $f$ increases, $Q_1$ is raised, whereas $Q_2$ is lowered $\forall \mu$. This means that some trade-off relationship exists between $Q_0$, $Q_1$, and $Q_2$. In the case of the classical absorber, a trade-off relation exists between two invariant points, which are independent of the absorber damping, and the optimal tuning is reached by equally leveling the invariant points. In this

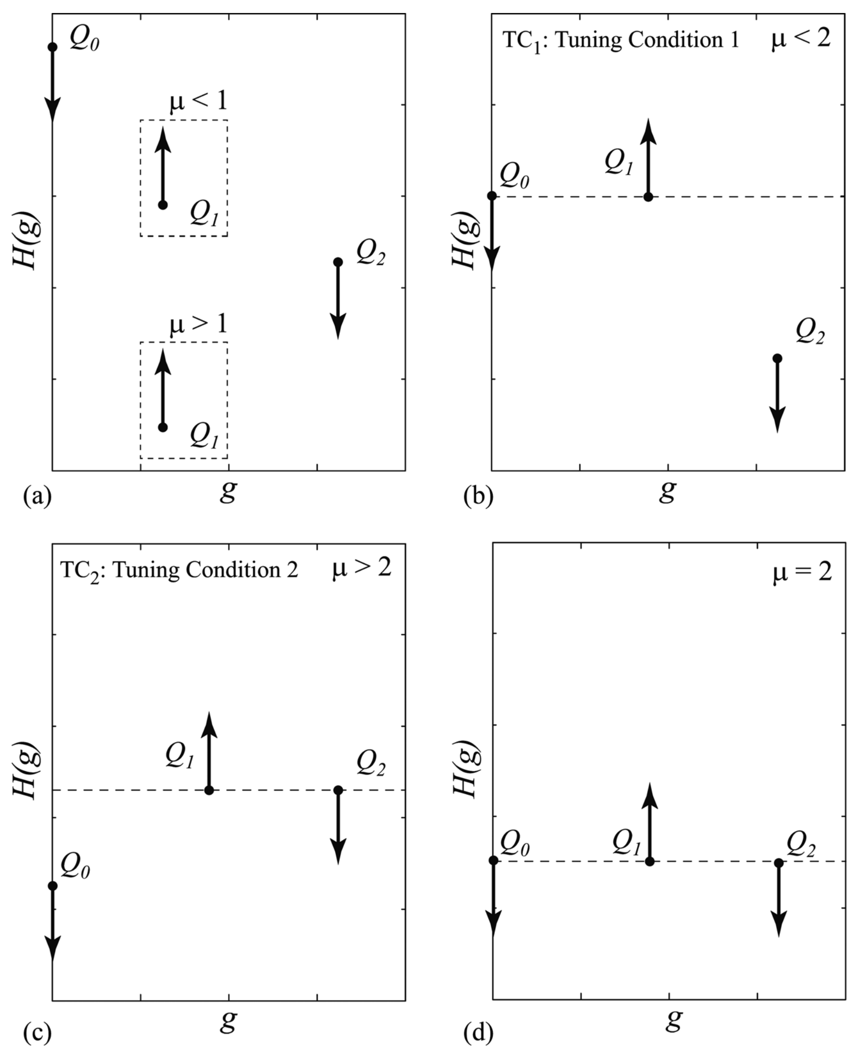


**Fig. 4 Positions of $Q_0$, $Q_1$, and $Q_2$ for different tuning ratios $f$. (*a*) Untuned $f=0$; (*b*) Tuned $f=f_{t_1}$; (*c*) Tuned $f=f_{t_2}$; and (*d*) Tuned $f=1/\sqrt{2}$.**

Downloaded from http://asmedigitalcollection.asme.org/vibrationacoustics/article-pdf/135/5/051003/6342559/vib_135_5_051003.pdf by guest on 29 May 2023

problem, and since $Q_1$ always moves in a direction opposite to that of $Q_0$ and $Q_2$ as $f$ varies, two trade-off relations exist: one between $Q_1$ and $Q_0$ and another one between $Q_1$ and $Q_2$, depending on the value of mass ratio $\mu$. Consider the case where $\mu \leq 1$; by inspecting Fig. 4(*a*), $Q_1$ is higher than or equal to the level of $Q_2$, and as $f$ varies, optimal tuning is reached when $Q_0$ and $Q_1$ meet at the same level. At this point, $Q_2$ is lower than the $Q_1$–$Q_0$ level and the system is properly tuned. Now, when $\mu > 1$, two scenarios are possible. In the first, since $Q_1$ is lower than $Q_2$, as $f$ is increased, the two points will meet at some level. If, at that state, $Q_0$ is lower than the $Q_1$–$Q_2$ level, the system is properly tuned. If not, tuning is achieved by further increasing $f$ so that $Q_1$ and $Q_0$ meet at the same level. Thus, the optimal tuning ratio will be calculated from two different tuning conditions defined as follows:

**Tuning condition 1** ($TC_1$): adjusting $Q_1$ and $Q_0$ to the same height and ensuring that $Q_2$ is lower than the $Q_0$–$Q_1$ level. This scenario is depicted in Fig. 4(*b*).
**Tuning condition 2** ($TC_2$): adjusting $Q_1$ and $Q_2$ to the same height and ensuring that $Q_0$ is lower than the $Q_1$–$Q_2$ level. This scenario is depicted in Fig. 4(*c*).

The choice of the correct tuning condition depends on the mass ratio $\mu$. After calculating the optimal tuning ratio, the optimal damping is obtained by forcing $H(g)$ not to exceed the $Q_0$–$Q_1$ or $Q_1$–$Q_2$ level. In Sec. 4, the optimal tuning ratios are obtained in analytical closed forms in terms of $\mu$.

## 4 Optimal Tuning

Let $f_{t_1}$ denote the optimal tuning ratio associated with $TC_1$ (i.e., $Q_0$ and $Q_1$ being at the same level). It is calculated from the equation

$$H(g_0) = H(g_1) \tag{5}$$

Solving Eq. (5) (see Appendix A.3) yields

$$f_{t_1} = \sqrt{\frac{9 + 12\mu - 3(3s)^{\frac{1}{3}} + (3s)^{\frac{2}{3}}}{6\mu(3s)^{\frac{1}{3}}}} \\ s = 9 - 18\mu + 2\sqrt{-3\mu(54 + \mu(9 + 16\mu))} \tag{6}$$

Similarly, the tuning ratio $f_{t_2}$, for which $TC_2$ is satisfied, is calculated from the below equation,

$$H(g_1) = H(g_2) \tag{7}$$

which yields (see Appendix A.4)

$$f_{t_2} = \sqrt{\frac{\mu - 1}{\mu}} \tag{8}$$

It is easily deduced from Eq. (8) that $f_{t_2}$ is only valid for $\mu \geq 1$. This means that, when $\mu < 1$, $Q_1$ and $Q_2$ will never meet. This was expected, since, as discussed before, when $f = 0$ and for $\mu < 1$, $Q_1$ starts at a level higher than that of $Q_2$. Furthermore, as $f$ increases, $Q_1$ moves upwards, whereas $Q_2$ moves downwards and, hence, these points will never meet. Now, to ensure that the system is properly tuned, $Q_2$ should be lower than the $Q_0$–$Q_1$ level when $f = f_{t_1}$ and $Q_0$ should be lower than the $Q_1$–$Q_2$ level when $f = f_{t_2}$. The range of $\mu$ over which $TC_2$ is satisfied is calculated first. When $f = f_{t_2}$, the level of $Q_0$ is calculated from $H(g_0)$ and the $Q_1$–$Q_2$ level from $H(g_1)$ or $H(g_2)$ as

$$H(g_0)|_{f=f_{t_2}} = \frac{\mu}{\mu - 1}$$
$$H(g_1)|_{f=f_{t_2}} = \sqrt{2\mu}$$

Solving the below inequality yields the domain of definition of $TC_2$,

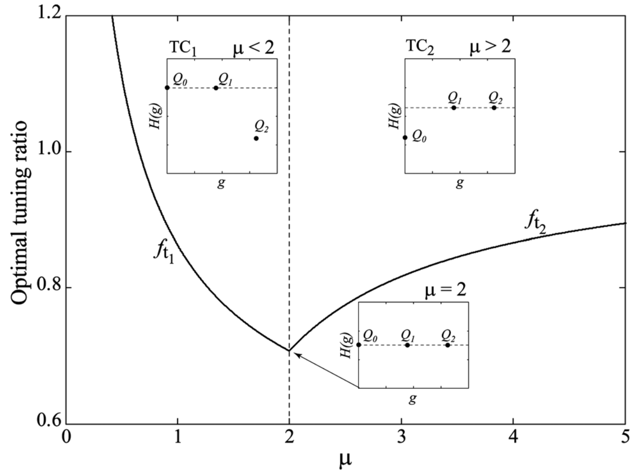

**Fig. 5 Plot of the optimal tuning ratio calculated from $f_{t_1}$ and $f_{t_2}$**

$$H^2(g_0)|_{f=f_{t_2}} < H^2(g_1)|_{f=f_{t_2}} \tag{9}$$

It is shown in Appendix A.5 that Eq. (9) is verified $\forall \mu > 2$. Finally, if $f = f_{t_2}$ and $\mu > 2$, the two points $Q_1$ and $Q_2$ will be at the same level and $Q_0$ lower than that level, thus satisfying $TC_2$. This case is depicted in Fig. 4(*c*). The domain of definition of $TC_1$ (i.e., $0 < \mu < 2$) is simply the complement of $\mu > 2$. Similarly, when $f = f_{t_1}$ and $0 < \mu < 2$, $Q_0$ and $Q_1$ will become equally leveled and $Q_2$ lower than that level, as shown in Fig. 4(*b*). It is important to note that, when $\mu = 2, f_{t_1} = f_{t_2} = 1/\sqrt{2}$ and optimal tuning corresponds to all three points, namely, $Q_0$, $Q_1$, and $Q_2$ being at the same level. This scenario is illustrated in Fig. 4(*d*). The optimal tuning ratio is plotted in Fig. 5, in which the plot is split into two parts. The first corresponds to $0 < \mu < 2$, where $TC_1$ holds and $f_{t_1}$ is plotted, and the second part of the plot corresponds to $\mu > 2$, where $TC_2$ holds and $f_{t_2}$ is plotted. Figure 5 clearly shows that the lowest optimal tuning ratio corresponds to $\mu = 2$ and is equal to $1/\sqrt{2}$. When the platform mass is equal to zero (i.e., $\mu = 0$), the stiffness $K$ of the primary system becomes directly connected in series with a resilient element comprised of the platform spring $k$ and damper $c$. On the limit, $f_{t_1}$ tends towards infinity as $\mu$ tends towards zero. Now, when $m$ is too large, the main mass can be assumed to be connected directly to the ground through the spring $K$. On the limit, $f_{t_2}$ tends to one as $\mu$ tends towards infinity.

## 5 Optimal Damping

**5.1 Tuning Condition 1:** $TC_1, f = f_{t_1}$ and $0 < \mu < 2$. After calculating the optimal tuning ratio $f_{t_1}$ defined for $0 < \mu < 2$ by equally leveling $Q_0$ and $Q_1$, the optimal damping ratio is determined such that the $Q_0$–$Q_1$ level is not exceeded by $H(g)$. The system considered has two degrees of freedom, and thus, its frequency response function is expected to have at most two peaks, corresponding to the system damped resonant frequencies. Since $Q_0$ and $Q_1$ are independent of $\zeta$, the best choice of the latter would be that resulting in $H(g)$, with two peaks coinciding with $Q_0$ and $Q_1$. In this case, the frequency response function will not exceed the $Q_0$–$Q_1$ level $\forall g$, thus resulting in an exact optimal solution to the problem. To better visualize the optimal configuration of $H(g)$, Fig. 6 shows $H(g)$ for $\mu = 0.8, f_{t_1} = 0.93$, and three different values of $\zeta$. The optimal configuration of $H(g)$ corresponds to $\zeta_3 = 1.23$, where $Q_0$ and $Q_1$ are its two maxima. Two other non-optimal shapes of $H(g)$ corresponding to $\zeta_1 = 1.3$ and $\zeta_2 = 1.1$ are shown.

It can be easily shown that the slope of $H(g)$ at $g_0$ is equal to zero, $\forall \mu, \forall f$, and $\forall \zeta$. Therefore, the optimal damping ratio $\zeta_{opt_{1a}}$ is obtained by forcing $H(g)$ to pass horizontally through $Q_1$. $\zeta_{opt_{1a}}$ is



Downloaded from http://asmedigitalcollection.asme.org/vibrationacoustics/article-pdf/135/5/051003/6342559/vib_135_5_051003.pdf by guest on 29 May 2023

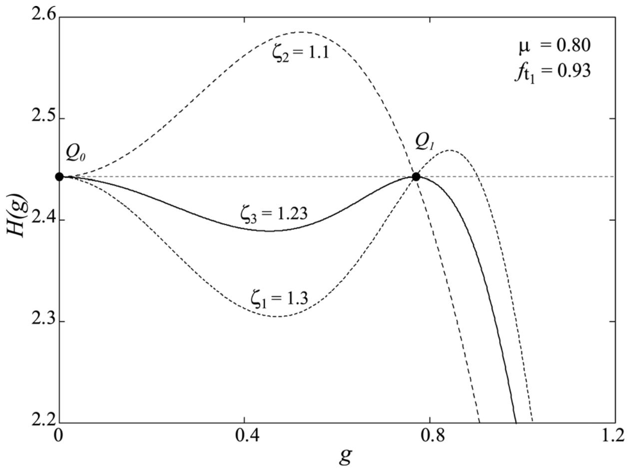


**Fig. 6 Plots of $H(g)$ in its optimal shape for $\zeta_3 = 1.23$ and in two other nonoptimal shapes for $\zeta_1 = 1.3$ and $\zeta_2 = 1.1$**

calculated analytically in Appendix A.6 using the perturbation method adopted in Ref. [4] as

$$\zeta^2_{\text{opt}_{1a}} = \frac{4f^4_{t_1}\mu^2 - 4f^2_{t_1}\mu^2 + f^2_{t_1}\mu - 3}{8\left(2f^6_{t_1}\mu^3 - 2f^4_{t_1}\mu^3 + 3f^4_{t_1}\mu^2 - f^2_{t_1}\mu^2 - 1\right)} \tag{10}$$

Equation (10) ensures that $H(g)$ will pass horizontally through $Q_1$ without asserting if the latter is a maximum or a minimum of $H(g)$. Similarly, $\forall\,\zeta$, $H(g)$ passes horizontally through $Q_0$, which can be either a maximum or a minimum. The optimal solution is achieved when both points are peaks of $H(g)$, and thus, the second derivative of $H(g)$ with respect to $g$ (i.e., $\partial_{g,g}H(g)$) should be negative at both $Q_0$ and $Q_1$.

$$\partial_{g,g}H(g_0)|_{f=f_{t_1},\zeta=\zeta_{\text{opt}_{1a}}} \le 0, \quad \partial_{g,g}H(g_1)|_{f=f_{t_1},\zeta=\zeta_{\text{opt}_{1a}}} \le 0 \tag{11}$$

The range of $\mu$ for which the inequalities in Eq. (11) are satisfied cannot be obtained analytically, because the expressions of $\partial_{g,g}H(g_0)$ and $\partial_{g,g}H(g_1)$ are too complicated. An alternative numerical approach is used, where $\partial_{g,g}H(g_0)$ and $\partial_{g,g}H(g_1)$ are plotted in Fig. 7 in the range $0 < \mu \le 2$. Figure 7(*a*) indicates that $Q_0$ is a peak for $0 < \mu \le 0.954$ and Fig. 7(*b*) that $Q_1$ is a peak for $0 < \mu \le 1.106$. When $0.954 \le \mu \le 1.106$, $Q_0$ is a minimum and $Q_1$ a maximum. This case is illustrated in Fig. 8(*a*), where $\mu = 1.0$. When $1.106 \le \mu < 2$, both $Q_0$ and $Q_1$ are minima; this case is depicted in Fig. 8(*b*), where $\mu = 1.5$. Finally, it is concluded that the optimal damping ratio $\zeta_{\text{opt}_{1a}}$ yields an optimal solution for the range $0 \le \mu \le 0.954$ only, where both $Q_0$ and $Q_1$ are maxima.

Let $\zeta_{\text{opt}_{1b}}$ denote the optimal damping ratio in the range $0.954 \le \mu \le 2$; it will be derived using a new constraint on the shape of $H(g)$. The optimal configuration of $H(g)$ in the range $0.954 \le \mu \le 2$ is determined by observing the behavior of its two peaks as $\zeta$ is varied. Let $g_A$ and $g_B$ denote the frequency ratios at these peaks. It is observed that a trade-off relation exists between the peaks $H(g_A)$ and $H(g_B)$, similar to that which exists between the invariant points $Q_0$–$Q_1$ and $Q_1$–$Q_2$. After tuning the system, and as $\zeta$ is varied, the peaks move in opposite directions, and thus, the optimal design corresponds to the two peaks being at the same level. Therefore, $\zeta_{\text{opt}_{1b}}$ can be calculated from the following equation:

$$H^2(g_A)|_{f=f_{t_1}} = H^2(g_B)|_{f=f_{t_1}} \tag{12}$$

In the process of calculating the optimal damping ratio $\zeta_{\text{opt}_{1b}}$, $g^2$ is replaced by $G$ and $H^2(G)$ is written as the ratio of two polynomials $N(G)$ and $D(G)$ as

$$H^2(G) = \frac{N(G)}{D(G)} \tag{13}$$

N$(G)$ and $D(G)$ are deduced from Eq. (4) and take the form

$$\begin{aligned} N(G) &= \left(1 + f^2\mu - G\mu\right)^2 + 4G\mu^2\zeta^2 \\ D(G) &= \left((1-G)(f^2 - G)\mu - G\right)^2 + 4G(1-G)^2\mu^2\zeta^2 \end{aligned} \tag{14}$$

Let $G_A = g_A^2, G_B = g_B^2$, and $L = H^2(G_A) = H^2(G_B)$. When $H(G)$ assumes its optimal configuration (i.e., when $H^2(G_A) = H^2(G_B)$), the following two equations hold for $G = G_A$ and $G = G_B$:

$$\begin{aligned} &N(G)/D(G) - L = 0 \\ &\frac{N'(G)\,D(G) - N(G)\,D'(G)}{D^2(G)} = 0 \end{aligned} \tag{15}$$

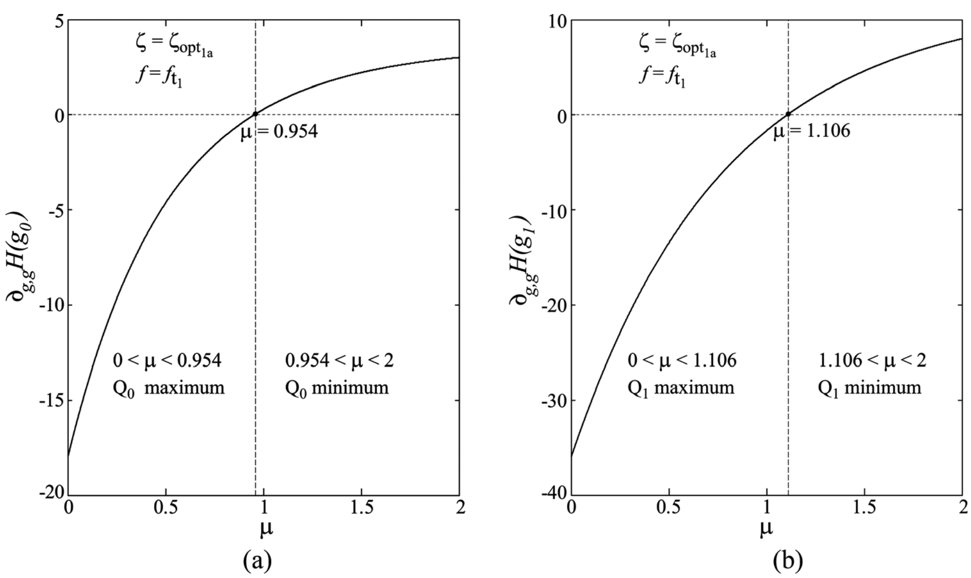


**Fig. 7 Plots of $\partial_{g,g}H(g)$ at $g_0$ and $g_1$ showing the range of $\mu$, in which $Q_0$ and $Q_1$ are maxima or minima. (*a*) $\partial_{g,g}H(g_0)$; and (*b*) $\partial_{g,g}H(g_1)$.**



Downloaded from http://asmedigitalcollection.asme.org/vibrationacoustics/article-pdf/135/5/051003/6342559/vib_135_5_051003.pdf by guest on 29 May 2023

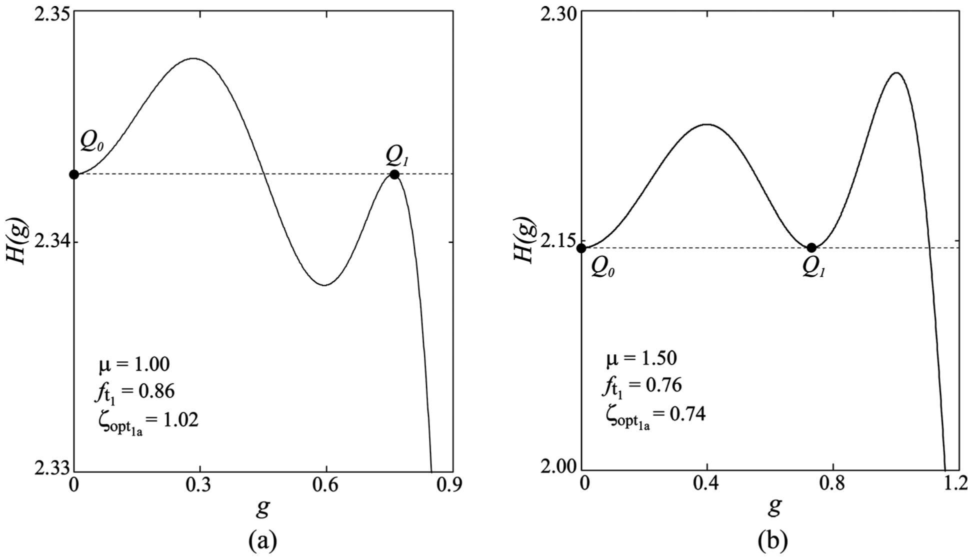


**Fig. 8 Plots showing cases where $\zeta_{\mathrm{opt}_{1a}}$ fails to yield an optimal solution. (*a*) $Q_0$ minimum and $Q_1$ maximum; and (*b*) $Q_0$ minimum and $Q_1$ minimum.**

$\square'$ denotes the partial derivative of $\square$ with respect to $G$. After simplification, the equations in Eq. (15) are simplified to

$$\begin{aligned} N(G) - LD(G) &= 0 \\ N'(G) - LD'(G) &= 0 \end{aligned} \tag{16}$$

Define the function $F(G) = N(G) - LD(G)$; then, it is concluded from Eq. (16) that $F(G) = 0$ will have two double roots at $G = G_A$ and $G = G_B$ when $H(G)$ assumes its optimal shape. $F(G)$ is a fourth order polynomial in $G$, which takes the form

$$\begin{aligned} F(G) &= N(G) - LD(G) \\ F(G) &= b_0\left(G^4 + b_1 G^3 + b_2 G^2 + b_3 G + b_4\right) \end{aligned} \tag{17}$$

where

$$\begin{aligned} b_0 &= -L\mu^2, \\ b_1 &= 4\zeta^2 - 2 - 2f_{t_1}^2 - 2/\mu, \\ b_2 &= 1 + f_{t_1}^4 - 1/L - 8\zeta^2 + 4f_{t_1}^2 + 2f_{t_1}^2/\mu + 1/\mu^2 + 2/\mu, \\ b_3 &= -2\left(f_{t_1}^4 L\mu - 2(L-1)\zeta^2\mu + f_{t_1}^2(L - \mu + L\mu) - 1\right)/(L\mu), \\ b_4 &= \left(f_{t_1}^4 (L-1)\mu^2 - 2f_{t_1}^2\mu - 1\right)/(L\mu^2) \end{aligned} \tag{18}$$

Since $G_A$ and $G_B$ are double roots of $F(G) = 0$, then $F(G)$ can be factorized as

$$F(G) = b_0 (G - G_A)^2 (G - G_B)^2 \tag{19}$$

Expanding Eq. (19) and comparing it to Eq. (17) leads to the following coefficients:

$$\begin{aligned} b_1 &= -2(G_A + G_B), \\ b_2 &= G_A^2 + 4G_A G_B + G_B^2, \\ b_3 &= -2G_A G_B (G_A + G_B), \\ b_4 &= G_A^2 G_B^2 \end{aligned} \tag{20}$$

Two equations relating the coefficients $b_i, (i = 1, \ldots, 4)$ are deduced from Eq. (20) by eliminating $G_A$ and $G_B$ as

$$\begin{aligned} b_1\sqrt{b_4} - b_3 &= 0 \\ b_1^2/4 + 2\sqrt{b_4} - b_2 &= 0 \end{aligned} \tag{21}$$

The unknowns of the two equations in Eq. (21) are the optimal damping constant $\zeta_{\mathrm{opt}_{1b}}$ and $L$. A closed form solution of $\zeta_{\mathrm{opt}_1 b}$ is not possible in this case, and thus, the latter is calculated numerically by solving these two nonlinear equations for a given $\mu$. The method used in the calculation of $\zeta_{\mathrm{opt}_{1b}}$ was first presented in Ref. [7] and used for the calculation of the exact optimal parameters of the classical vibration absorber.

### 5.2 Tuning Condition 2: $\mathrm{TC}_2, f = f_{t_2}$ and $\mu \geq 2$.

The second tuning condition corresponding to $f = f_{t_2}$ is valid $\forall \mu \geq 2$, where $Q_1$ and $Q_2$ are equally leveled and $Q_0$ is below that level. Similar to the previous case, the exact optimal solution can be attained if $H(g)$ assumes $Q_1$ and $Q_2$ as its peaks. It can be shown that this cannot be achieved, and hence, a semiexact analytical solution is obtained by equally leveling the peaks of $H(g)$. Let $\zeta_{\mathrm{opt}_2}$ denote the optimal damping ratio; it is obtained from Eq. (21) by replacing $f_{t_1}$ by $f_{t_2}$. Unlike $f_{t_1}$, the expression of $f_{t_2}$ (i.e., $\sqrt{(\mu-1)/\mu}$) is relatively simple. Substituting $f_{t_2}$ into Eq. (21) yields two nonlinear equations in $\zeta_{\mathrm{opt}_2}$ and $L$. These equations are solved analytically, and a closed form solution of $\zeta_{\mathrm{opt}_2}$ is obtained as follows:

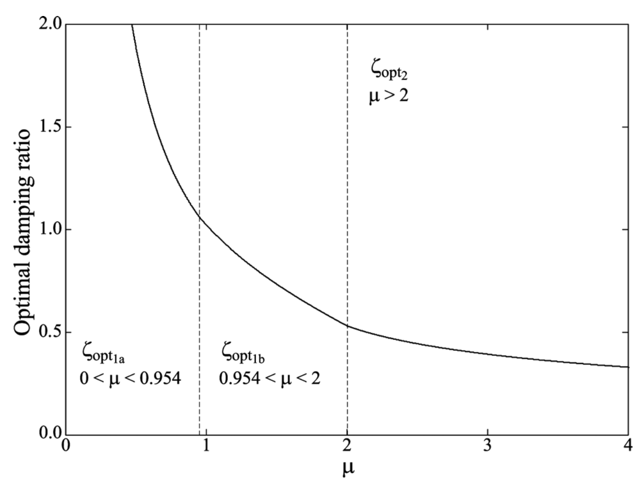


**Fig. 9 Plot of the optimal damping ratio**



Downloaded from http://asmedigitalcollection.asme.org/vibrationacoustics/article-pdf/135/5/051003/6342559/vib_135_5_051003.pdf by guest on 29 May 2023

**Table 1 Optimal parameters of the viscously damped vibration absorber (platform)**

| | $0 \le \mu \le 2$ | | $2 \le \mu \le \infty$ |
|---|---|---|---|
| Optimal tuning | $f_{t_1} = \sqrt{\dfrac{9+12\mu-3(3s)^{\frac{1}{3}}+(3s)^{\frac{2}{3}}}{6\mu(3s)^{\frac{1}{3}}}}$, | $s = 9-18\mu+2\sqrt{-3\mu(54+\mu(9+16\mu))}$ | $f_{t_2} = \sqrt{\dfrac{\mu-1}{\mu}}$ |
| | $0 \le \mu \le 0.954$ | $0.954 \le \mu \le 2$ | $q^3 = 3\sqrt{3\mu(208+\mu(128\mu-325))-144}+117\mu-184$ |
| Optimal damping | $\zeta^2_{\text{opt}_{1a}} = \dfrac{4f_{t_1}^4\mu^2-4f_{t_1}^2\mu^2+f_{t_1}^2\mu-3}{8(2f_{t_1}^6\mu^3-2f_{t_1}^4\mu^3+3f_{t_1}^4\mu^2-f_{t_1}^2\mu^2-1)}$ | $\zeta_{\text{opt}_{1b}}$ is the solution of : $b_1\sqrt{b_4}-b_3=0$; $b_1^2/4+2\sqrt{b_4}-b_2=0$ | $r = \sqrt{\dfrac{\sqrt[3]{2}\,q^2+(3\mu-8)\,q+2\sqrt[3]{4}(13-6\mu)}{12\,\mu\,q}}$; $\zeta_{\text{opt}_2} = \sqrt{\dfrac{1}{4}+\dfrac{1}{2}r-\dfrac{1}{2}\sqrt{\dfrac{(3\mu-8)}{4\mu}+\dfrac{1}{4r}-r^2}}$ |

$$q^3 = 3\sqrt{3\mu(208+\mu(128\mu-325))-144}+117\mu-184$$
$$r = \sqrt{\frac{\sqrt[3]{2}\,q^2+(3\mu-8)\,q+2\sqrt[3]{4}(13-6\mu)}{12\,\mu q}} \tag{22}$$
$$\zeta_{\text{opt}_2} = \sqrt{\frac{1}{4}+\frac{1}{2}r-\frac{1}{2}\sqrt{\frac{(3\mu-8)}{4\mu}+\frac{1}{4r}-r^2}}$$

The optimal damping ratio is plotted in Fig. 9. The range of $\mu$ is split into three parts, where $\zeta_{\text{opt}_{1a}}$, $\zeta_{\text{opt}_{1b}}$, and $\zeta_{\text{opt}_2}$ are defined and plotted. The first two parts of the curve correspond to $f = f_{t_1}$ and the third to $f = f_{t_2}$. When the mass of the platform is zero, the primary system becomes directly connected to a resilient element made of the spring $k$ and damper $c$ of the platform. On the limit, as $\mu$ tends towards zero, $\zeta_{\text{opt}_{1a}}$ tends towards infinity. Finally, when the mass of the platform is too large, the primary system

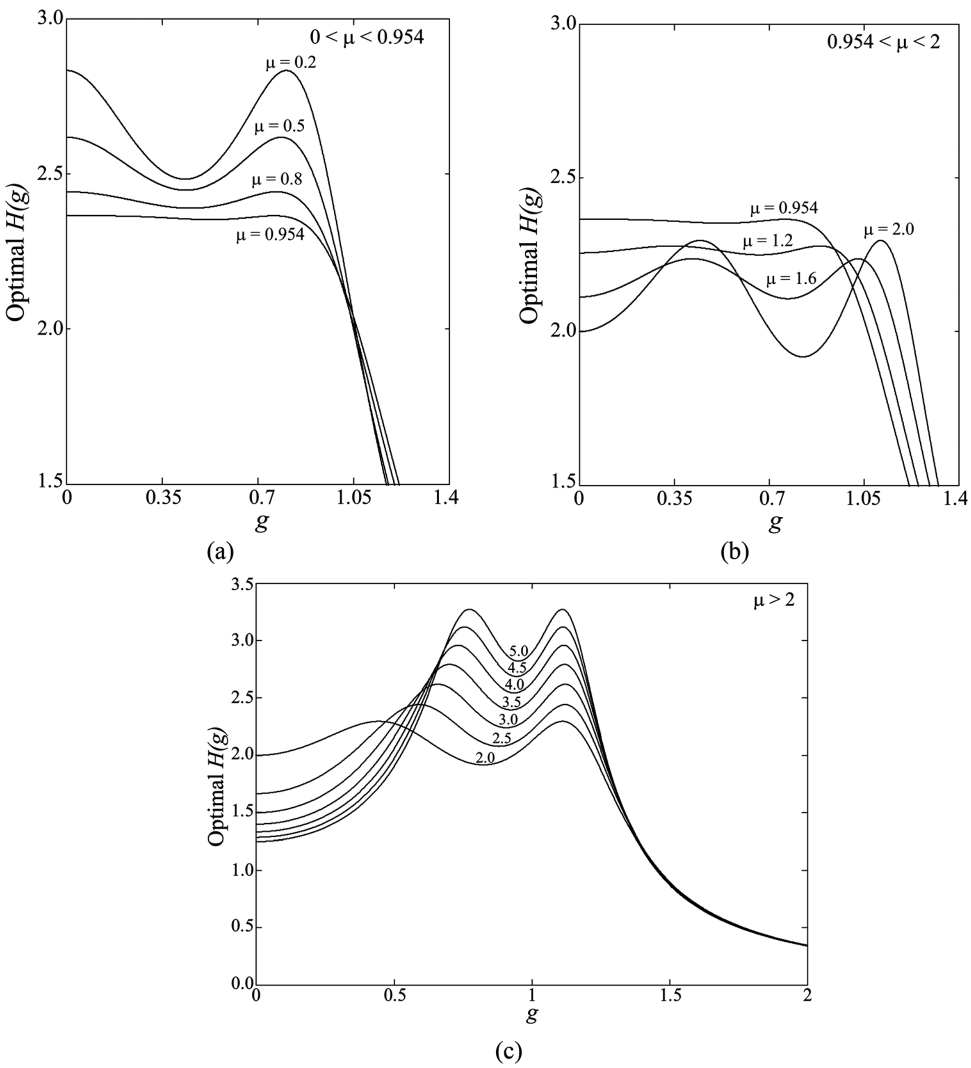


Fig. 10 Plots of the optimal shape of $H(g)$. (*a*) $f = f_{t_1}$ and $\zeta = \zeta_{\text{opt}_{1a}}$; (*b*) $f = f_{t_1}$ and $\zeta = \zeta_{\text{opt}_{1b}}$; and (*c*) $f = f_{t_2}$ and $\zeta = \zeta_{\text{opt}_2}$.



Downloaded from http://asmedigitalcollection.asme.org/vibrationacoustics/article-pdf/135/5/051003/6342559/vib_135_5_051003.pdf by guest on 29 May 2023

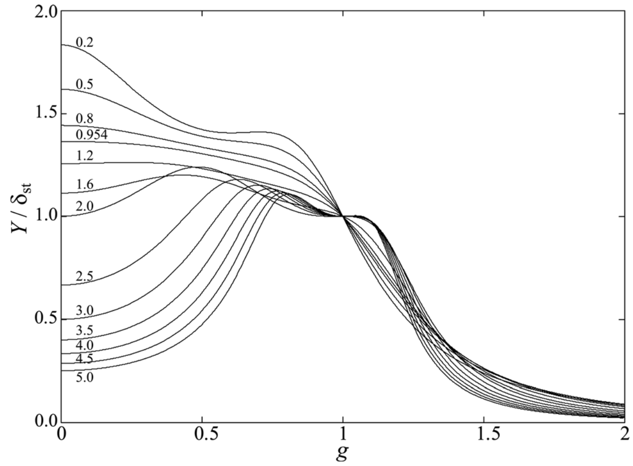


**Fig. 11 Plots of $Y/\delta_{st}$ using the optimal parameters**

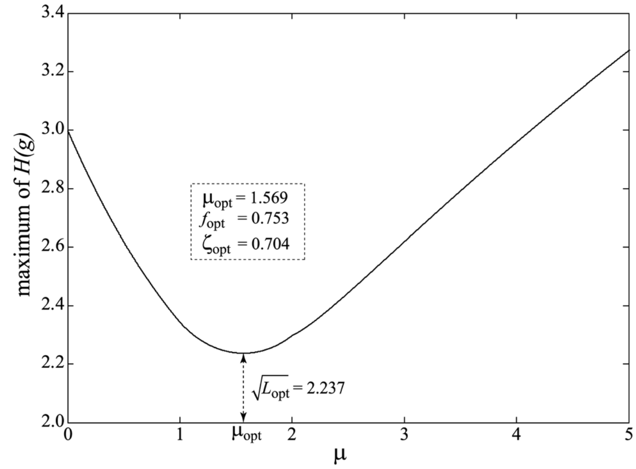


**Fig. 12 Plot of the maximum of $H(g)$, $\sqrt{L} = \|H(g)\|_{max}$**

becomes as if it is directly connected to the ground, and on the limit, as $\mu$ tends towards infinity, $\zeta_{opt_2}$ tends towards zero.

## 6 Discussion of Results

The optimal parameters of the platform absorber are determined using a method similar to that used by Den Hartog in the determination of the optimal parameters of the classical absorber. The optimal tuning and damping ratios are determined separately. The range of the mass ratio $\mu$ is split into two parts, and an optimal tuning ratio is calculated for each range. The first tuning condition, which corresponds to $f = f_{t_1}$ (Eq. (6)), holds for $0 < \mu \leq 2$, and the second tuning condition corresponds to $f = f_{t_2}$ (Eq. (8)) and holds for $\mu \geq 2$. Then, the optimal damping ratio is calculated such that the two peaks of $H(g)$ are at the same height. For $0 < \mu \leq 0.954$, a closed form expression for the optimal damping $\zeta_{opt_1a}$ is derived and the peaks coincided with the invariant points, yielding an exact solution to the problem. For $0.954 \leq \mu \leq 2$, the optimal damping $\zeta_{opt_{1b}}$ is calculated from Eq. (21). For $\mu \geq 2$, the optimal damping $\zeta_{opt_2}$ is obtained analytically as in Eq. (22). For $\mu \geq 0.954$, the equally leveled peaks do not coincide with the invariant points, and hence, the solution obtained is referred to as a semiexact solution. All design parameters are summarized in Table 1. The frequency response function $H(g)$ is plotted in Fig. 10 in its optimal shape for several values of the mass ratio $\mu$. Three figures are shown: the first two, namely Fig. 10(*a*) and Fig. 10(*b*), correspond to the first tuning condition, where $f = f_{t_1}$, and the two points $Q_0$ and $Q_1$ are at the same level. In Fig. 10(*a*), $\zeta = \zeta_{opt_{1a}}$, and the two peaks are at $Q_0$ and $Q_1$, yielding an exact optimal shape of $H(g)$, whereas, in Fig. 10(*b*), $\zeta = \zeta_{opt_{1b}}$, and the two peaks are at the same level, which is higher than the $Q_0$–$Q_1$ level, yielding a semiexact solution. Figure 10(*c*) illustrates several plots of $H(g)$ for $f = f_{t_2}$ and $\zeta = \zeta_{opt_2}$. In these curves, $Q_1$ and $Q_2$ are equally leveled and the $H(g)$ shapes are semiexact, since the two peaks are adjusted to the same height, which is higher than the $Q_1$–$Q_2$ level. The platform frequency response function is shown in Fig. 11 for all values of $\mu$ considered in the plots of Fig. 10. The figure clearly shows the existence of a fixed point at $g = 1$, yielding a unity magnification factor (i.e., $Y/\delta_{st} = 1$).

In this work, the optimal tuning and damping ratios are determined for a given mass ratio $\mu$ of the system. The same optimization problem was solved for the classical absorber setup in the literature, where it was shown that the maximum amplitude of the primary system decreases with increasing absorber mass. Hence, an optimal mass ratio does not exist in the classical setup case, in which performance increases with increasing mass ratio. As for the proposed absorber setup, the shapes of the frequency response functions shown in Fig. 10 clearly indicate the existence of an optimal mass ratio $\mu_{opt}$. In Fig. 10(*a*), as $\mu$ increases from zero, the height of the equally leveled peaks of $H(g)$ decreases. If $\mu$ is further increased from 0.954 to 2, as shown in Fig. 10(*b*), the height of the peaks' decreases reaches a minimum value and then increases back again. Hence, this indicates the existence of a minimum value of the peaks' height associated with the optimal mass ratio of the system $\mu_{opt}$. If $\mu$ is further increased beyond 2, the peaks' height will increase, as shown in Fig. 10(*c*). The maximum amplitude (peak's height) of the primary system is calculated and plotted in Fig. 12. For $0 < \mu \leq 0.954$, the maximum amplitude is simply equal to $H(0)$, since the peaks coincide with $Q_0$ and $Q_1$. For $\mu > 0.954$, it is equal to $\sqrt{L}$ and calculated from Eq. (21). The figure clearly shows the existence of a minimum that corresponds to $\mu_{opt} = 1.569, f_{t_1} = 0.753$, and $\zeta_{opt_{1b}} = 0.704$. The resultant lowest maximum amplitude of the primary system that can be achieved is equal to $2.237 \times \delta_{st}$. The frequency response functions of the primary system and platform associated with $\mu = \mu_{opt}$ are shown in Fig. 13. To achieve the optimal performance of the proposed absorber (i.e., $\| H(g) \|_{max} = 2.237$, using the classical setup, the absorber mass should equal 50% of the primary system mass (i.e., $\mu \approx 0.5$, as per Ref. [7]). Typically, the classical absorber mass is a small fraction of the primary system mass, and hence, $\mu \approx 0.5$ is too large to be considered an acceptable mass ratio for the classical setup (see Ref. [13]). Assuming that the primary system can withstand this heavy load, implementing an absorber with a mass equal to half of the primary system mass is a real hassle. Furthermore, some systems cannot even tolerate any loading on their external structures, and hence, for such systems, the proposed setup would be more appropriate than the classical one.

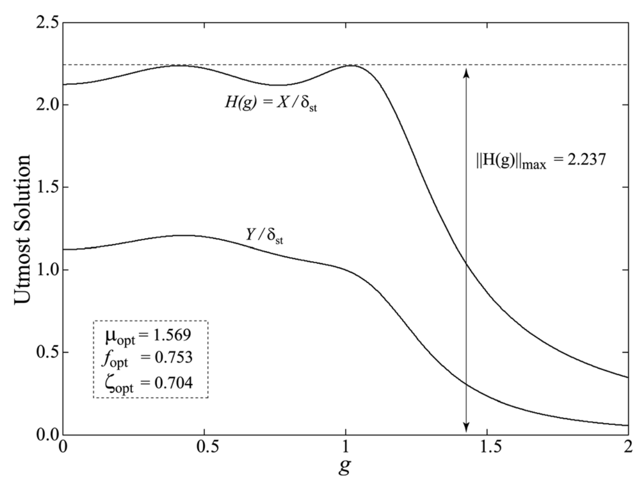


**Fig. 13 Plot of $H(g)$ and $Y/\delta_{st}$ for $\mu = \mu_{opt}$**



Downloaded from http://asmedigitalcollection.asme.org/vibrationacoustics/article-pdf/135/5/051003/6342559/vib_135_5_051003.pdf by guest on 29 May 2023

## 7 Conclusion

The optimal design of a viscously damped platform for vibration suppression in undamped single degree of freedom systems is proposed. For a given mass ratio $\mu$ of the system, the optimal tuning and damping ratios were determined with the aim of minimizing the maximum of the primary system frequency response. The solution was obtained by first setting two of three invariant points, which are independent of the damping ratio to equal heights, then by equally leveling the two peaks of the objective function. This was made possible due to the existence of a trade-off relation between the three invariant points and two peaks. Two different expressions of the optimal tuning ratio were determined analytically, each corresponding to a range of the mass ratio, where two of the three invariant points are set to equal heights. The range of $\mu$ over which the first tuning condition is defined is split into two subranges. In the first subrange, the optimal damping was determined analytically and led to the exact solution because the two peaks coincided with the equally leveled invariant points. The optimal damping corresponding to the second subrange is the solution of a nonlinear equation and led to a semiexact solution, where the two peaks do not coincide with the fixed points but are set to the same height. For the second tuning condition, a semiexact solution was obtained where the optimal damping ratio was determined analytically. It is shown that an optimal mass ratio $\mu_{opt}$ exists, unlike the case of the classical setup, where the absorber performance increases with its increasing mass.

## Appendix: Viscous Damping

**A.1 Frequency Ratios at the Fixed Points.** The frequency ratios at the fixed points are calculated by intersecting two $H(g)$ curves with different values of the damping ratio $\zeta$. For simplicity, the values $\zeta = 0$ and $\zeta = 1$ are chosen. The resultant equation is

$$H(g)^2|_{\zeta=0} = H(g)^2|_{\zeta=1}, \frac{(1+f^2\mu - g^2\mu)^2}{((1-g^2)(f^2-g^2)\mu - g^2)^2} = \frac{(1+f^2\mu-g^2\mu)^2+4g^2\mu^2}{((1-g^2)(f^2-g^2)\mu-g^2)^2+4g^2(1-g^2)^2\mu^2} \quad \text{(A1)}$$

Equation (A1) is reduced to the following third order polynomial in $g^2$:

$$2g^6\mu - 2g^4(1+\mu+f^2\mu) + g^2(1+2f^2\mu) = 0 \quad \text{(A2)}$$

Solving Eq. (A2) yields the frequency ratios at the three fixed points,

$$g_0 = 0, \quad g_1 = \sqrt{\frac{1+\mu+f^2\mu - \sqrt{(1+(f^2-1)\mu)^2+2\mu}}{2\mu}}, \quad g_2 = \sqrt{\frac{1+\mu+f^2\mu + \sqrt{(1+(f^2-1)\mu)^2+2\mu}}{2\mu}} \quad \text{(A3)}$$

**A.2 Variation of $H(g)$ With Respect to $f$ at $Q_0$, $Q_1$, and $Q_2$.** The objective function at the fixed points takes the form

$$\begin{aligned} H(g_0) &= \frac{1+f^2\mu}{f^2\mu} \\ H(g_1) &= \sqrt{(1+(f^2-1)\mu)^2+2\mu} + (1+(f^2-1)\mu) \\ H(g_2) &= \sqrt{(1+(f^2-1)\mu)^2+2\mu} - (1+(f^2-1)\mu) \end{aligned} \quad \text{(A4)}$$

Now, substituting $f=0$ in the above equations results in

$$\begin{aligned} H(g_0)|_{f=0} &= +\infty \\ H(g_1)|_{f=0} &= \sqrt{1+\mu^2} + (1-\mu) \\ H(g_2)|_{f=0} &= \sqrt{1+\mu^2} - (1-\mu) \end{aligned} \quad \text{(A5)}$$

It can be easily shown from Eq. (A5) that

$$\begin{aligned} H(g_1)|_{f=0} \le H(g_2)|_{f=0} < H(g_0)|_{f=0} \quad &\forall\ \mu \ge 1 \\ H(g_2)|_{f=0} < H(g_1)|_{f=0} < H(g_0)|_{f=0} \quad &\forall\ \mu < 1 \end{aligned}$$

Taking the derivatives of $H(g_0), H(g_1)$, and $H(g_2)$ with respect to $f$ results in

$$\begin{aligned} \frac{\partial H(g_0)}{\partial f} &= -\frac{2}{f^3\mu} \\ \frac{\partial H(g_1)}{\partial f} &= +\frac{2f\mu H(g_1)}{\sqrt{(1+(f^2-1)\mu)^2+2\mu}} \\ \frac{\partial H(g_2)}{\partial f} &= -\frac{2f\mu H(g_2)}{\sqrt{(1+(f^2-1)\mu)^2+2\mu}} \end{aligned} \quad \text{(A6)}$$

Since $H(g_1), H(g_2), f$, and $\mu$ are positive, then

$$\frac{\partial H(g_0)}{\partial f} < 0, \quad \frac{\partial H(g_1)}{\partial f} \ge 0, \quad \frac{\partial H(g_2)}{\partial f} \le 0 \quad \text{(A7)}$$

**A.3 TC$_1$—Optimal Tuning Ratio.** The optimal tuning ratio $f_{t_1}$ associated with TC$_1$ is calculated from the following equation:

$$H(g_0) = H(g_1) \quad \text{(A8)}$$

Substituting the expressions for $H(g_0)$ and $H(g_1)$ from Eqs. (A4) into (A8) yields, after simplification,

$$1+f^2\mu^2(1-f^2) - f^2\mu\sqrt{(1+(f^2-1)\mu)^2+2\mu} = 0 \quad \text{(A9)}$$

in which the solution yields $f_{t_1}$ as

$$f_{t_1} = \sqrt{\frac{9+12\mu-3(3s)^{\frac{1}{3}}+(3s)^{\frac{2}{3}}}{6\mu(3s)^{\frac{1}{3}}}}, \quad s = 9-18\mu+2\sqrt{-3\mu(54+\mu(9+16\mu))} \quad \text{(A10)}$$

**A.4 TC$_2$—Optimal Tuning Ratio.** The optimal tuning ratio corresponding to $Q_1$ and $Q_2$, being at the same level, is calculated from the equation

$$H(g_1) = H(g_2) \quad \text{(A11)}$$

Substituting the expressions for $H(g_1)$ and $H(g_2)$ from Eqs. (A4) into (A11) results in

$$2(1+(f^2-1)\mu) = 0 \quad \text{(A12)}$$

in which the solution yields $f_{t_2}$, the optimal tuning ratio associated with TC$_2$,

$$f_{t_2} = \sqrt{\frac{\mu-1}{\mu}} \quad \text{(A13)}$$

**A.5 TC$_2$—Domain of Definition.** The tuning condition TC$_2$ is defined when $Q_0$ is lower than the $Q_1$–$Q_2$ level, i.e.,

Downloaded from http://asmedigitalcollection.asme.org/vibrationacoustics/article-pdf/135/5/051003/6342559/vib_135_5_051003.pdf by guest on 29 May 2023

$$H^2(g_0)|_{f=f_{t_2}} < H^2(g_1)|_{f=f_{t_2}}$$

$$\frac{\mu^2}{(\mu-1)^2} < 2\mu \quad \text{(A14)}$$

$$\mu(2\mu-1)(\mu-2) > 0$$

The above inequality is valid $\forall\mu < 1/2$ or $\mu > 2$. The result $\mu < 1/2$ is rejected, since it does not verify $\mu \geq 1$. Hence, $TC_2$ is verified $\forall\mu > 2$.

**A.6 Optimal Damping: $\zeta_{opt_{1a}}$.** In order to force $H(g)$ to pass horizontally through $Q_1(g_1, H(g_1))$, the function is required first to pass through a point $Q_1'(g_1+\varepsilon, H(g_1))$, and then $\zeta$ is calculated from the limit as $\varepsilon$ tends towards zero. The damping ratio $\zeta$ is determined from Eq. (4) as

$$\zeta^2 = \frac{(1+f^2\mu-g^2\mu)^2 - H^2(g)\left((1-g^2)(f^2-g^2)\mu-g^2\right)^2}{4H^2(g)\,g^2(1-g^2)^2\mu^2-4g^2\mu^2} \quad \text{(A15)}$$

Substituting $g = g1+\varepsilon$ and $H(g) = H(g_1)$, the abscissa and ordinate of $Q_1'$ into this equation leads to an equation of the form

$$\zeta'^2 = \frac{A_0 + A_1\varepsilon + A_2\varepsilon^2 + \cdots}{B_0 + B_1\varepsilon + B_2\varepsilon^2 + \cdots} \quad \text{(A16)}$$

Since $Q_1$ is independent of $\zeta$, then $\varepsilon = 0$ should lead to the indeterminate form $\zeta^2 = A_0/B_0 = 0/0$ and thus $A_0 = B_0 = 0$. Finally the optimal damping ratio $\zeta_{opt_{1a}}$ is equal to

$$\zeta^2_{opt_{1a}} = \lim_{\varepsilon\to 0}\zeta'^2 = \frac{A_1}{B_1} = \frac{4f_{t_1}^4\mu^2 - 4f_{t_1}^2\mu^2 + f_{t_1}^2\mu - 3}{8(2f_{t_1}^6\mu^3 - 2f_{t_1}^4\mu^3 + 3f_{t_1}^4\mu^2 - f_{t_1}^2\mu^2 - 1)} \quad \text{(A17)}$$

## References


[1] Frahm, H., 1911, "Device for Damping Vibrations of Bodies," U.S. Patent No. 989,958.

[2] Ormondroyd, J., and Den Hartog, J. P., 1928, "The Theory of the Dynamic Vibration Absorber," ASME J. Appl. Mech., **50**, pp. 9–22.

[3] Den Hartog, J. P., 1940, *Mechanical Vibrations*, 2nd ed., McGraw-Hill, London.

[4] Brock, J. E., 1946, "A Note on the Damped Vibration Absorber," ASME J. Appl. Mech., **13**(4), p. A284.

[5] Den Hartog, J. P., 1985, *Mechanical Vibrations*, 4th ed., Courier Dover Publications, Mineola, NY, pp. 93–105.

[6] Rao, S. S., 2003, *Mechanical Vibrations*, 4th ed., Prentice-Hall, Upper Saddle River, NJ, pp. 710–714.

[7] Nishihara, O., and Asami, T., 2002, "Closed-Form Solutions to the Exact Optimizations of Dynamic Vibration Absorbers (Minimizations of the Maximum Amplitude Magnification Factors)," ASME J. Vib. Acoust., **124**(4), pp. 576–582.

[8] Snowdon, J. C., 1959, "Steady-State Behavior of the Dynamic Absorber," J. Acoust. Soc. Am., **31**(8), pp. 1096–1103.

[9] Ozer, M. B., and Royston, T. J., 2005, "Extending Den Hartog's Vibration Absorber Technique to Multi-Degree-of-Freedom Systems," ASME J. Vib. Acoust., **127**(4), pp. 341–350.

[10] Asami, T., and Nishihara, O., 2003, "Closed-Form Exact Solution to $h_\infty$ Optimization of Dynamic Vibration Absorbers (Application to Different Transfer Functions and Damping Systems)," ASME J. Vib. Acoust., **125**(3), pp. 398–405.

[11] Bapat, V. A., and Kumaraswamy, H. V., 1979, "Effect of Primary System Damping on the Optimum Design of an Untuned Viscous Dynamic Vibration Absorber," J. Sound Vib., **63**(4), pp. 469–474.

[12] Thompson, A. G., 1981, "Optimum Tuning and Damping of a Dynamic Vibration Absorber Applied to a Force Excited and Damped Primary System," J. Sound. Vib., **77**(3), pp. 403–415.

[13] Randall, S. E., Halsted, D. M., and Taylor, D. L., 1981, "Optimum Vibration Absorbers for Linear Damped Systems," ASME J. Mech. Des., **103**(4), pp. 908–913.

[14] Soom, A., and Lee, M. S., 1983, "Optimal Design of Linear and Nonlinear Vibration Absorbers for Damped Systems," ASME J. Vib. Acoust., **105**, pp. 112–119.

[15] Pennestri, E., 1998, "An Application of Chebyshev's Min-Max Criterion to the Optimal Design of a Damped Dynamic Vibration Absorber," J. Sound Vib., **217**(4), pp. 757–765.

[16] Febbo, M., and Vera, S. A., 2008, "Optimization of a Two Degree of Freedom System Acting as a Dynamic Vibration Absorber," ASME J. Vib. Acoust., **130**(1), p. 011013.

[17] Febbo, M., 2012, "Optimal Parameters and Characteristics of a Three Degree of Freedom Dynamic Vibration Absorber," ASME J. Vib. Acoust., **134**(2), p. 021010.


Downloaded from http://asmedigitalcollection.asme.org/vibrationacoustics/article-pdf/135/5/051003/6342559/vib_135_5_051003.pdf by guest on 29 May 2023